A Bootstrap Method for Sinusoid Detection in Colored Noise and Uneven Sampling. Application to Exoplanet Detection

Sophia Sulis, David Mary, Lionel Bigot

Université Côte d'Azur, Observatoire de la Côte d'Azur, Laboratoire Lagrange,
UMR CNRS 7293, CS 34229, 06304 Nice, France

ABSTRACT

This study is motivated by the problem of evaluating reliable false alarm (FA) rates for sinusoid detection tests applied to unevenly sampled time series involving colored noise, when a (small) training data set of this noise is available. While analytical expressions for the FA rate are out of reach in this situation, we show that it is possible to combine specific periodogram standardization and bootstrap techniques to consistently estimate the FA rate. We also show that the procedure can be improved by using generalized extreme-value distributions. The paper presents several numerical results including a case study in exoplanet detection from radial velocity data.

Index Terms— Bootstrap, colored noise, detection.

I. INTRODUCTION

This study is motivated by the problem of assessing reliable false alarm (FA) rates for detection tests when the noise is colored, with partially unknown statistics and when the sampling is not regular. Sinusoid (or more generally periodicity) detection tests are often based on the (Schuster's) periodogram [1], defined as

$$P(\nu) := \frac{1}{N} \left| \sum_{j=1}^{N} X(t_j) e^{-i2\pi\nu t_j} \right|^2, \quad (1)$$

with $\{X(t_j)\}_{j=1,\ldots,N}$ the data samples and ν the frequency. In the case of uneven time sampling, which is of concern in the present study, the periodogram ordinates in (1) are not independent, even when the noise is white Gaussian, because the sampled exponentials are not orthogonal in general [2]. This dependence makes the analysis of FA rates difficult.
In the literature of periodicity detection, numerous "generalized" periodograms (i.e., different from (1)) have been proposed (*e.g.*, [2], [3]), which correlate the time series with (possibly highly redundant) dictionaries of target signatures. As for Schuster's periodogram however, owing to at least one of the three following factors :
(i) uneven sampling,
(ii) intrinsic correlation of the considered features,
(iii) partially unknown noise correlations or dependencies,
the joint distribution of these periodogram ordinates is unknown (although the marginal distribution can be obtained

in some cases), which prevents from deriving accurate false FA rates (see [4]). Empirical methods exist (*e.g.*, [5]) but they often lead to inconsistencies [4], [6]. To the best of our knowledge, the problem of accurately estimating the FA rate of periodograms-based detection tests in the case of uneven sampling and partially unknown colored noise remains open. Yet, the case of irregular sampling is frequently encountered in practice, for instance in astronomical observations [2], [4]. The present study explores a bootstrap solution to this problem. As in [7], we assume that a training data set $\mathcal{T}_L$ of the noise is available. However, this set provides only a *small* number of noise samples - comparable typically to the number of data samples. In this regime, our knowledge of the statistics of the random process under $\mathcal{H}_0$ remains strongly impacted by estimation noise. The working hypothesis of an available training data set is rather general, but arises in particular in the field of exoplanet detection in Radial Velocity (RV) data, where astrophysical models allow to generate time series of the noise - yet at a computational cost that makes long simulated time series out of reach. We show in the end of the paper that accurate estimates of the FA rate can nevertheless be obtained in such conditions, at least for some tests. To do so, our strategy will be to cancel the nuisances caused by the unknown noise statistics by considering standardized periodograms, for which the $\{t_j\}$ in (1) are unevenly spaced, and to capture the dependencies between the periodogram ordinates through bootstrap techniques.

In essence, the bootstrap is a computational tool for statistical inference using sample-driven Monte Carlo (MC) simulations to produce empirical estimates of several statistical quantities as, here, the periodogram distribution and estimates of the FA rates [8]. These techniques, initially introduced for independent and identically distributed random variables (r.v.), have been intensively studied in the last decades [8]. Bootstrap techniques exist in the case of even sampling and weakly dependent data (*e.g.*, [9]) and different resampling procedures have been proposed (*e.g.*, [10]). For longer memory processes, autoregressive (AR)-aided periodogram bootstrap consists in estimating the parameters of an AR model in the time domain and in applying a non-parametric kernel based correction in the frequency domain to counteract the effects of estimation noise on the

AR parameters (*e.g.*, [11]). For the uneven sampling case, "dependent wild bootstrap" adapted to weakly dependent data unevenly sampled can be found in [12] and a bootstrap procedure using a Generalized Extreme Value (GEV) fit on the periodogram maxima is presented in [4]. As underlined in [13] for instance, the choice of the parameters of such procedures (*e.g.*, parametric noise models, number of blocks, block lengths, data weights or repartition of the sampled blocks) can be delicate.

To conclude this short review of a large literature, controlling the FA rate in sinusoid detection is problematic in the case of an uneven sampling and partially unknown colored noise, even when resorting to bootstrap techniques.

In this study, we renounce to obtain analytical expressions of the P_{FA}. The contributions are the following : in Sec.II and Sec.III, we propose an original and automated bootstrap method based on a parametric-aided periodogram allied to periodogram standardization. In Sec.IV, we propose to take advantage from GEV distributions to improve the method and, in Sec.V, we present some of our numerical results, including an application to exoplanet detection.

II. STANDARDIZED PERIODOGRAM AND STATISTICAL TEST

Let us consider an observed time series of Power Spectrum Density (PSD) S, noted $X_{obs}|S$, involving a random process (with unknown PSD S_E), plus possibly a periodic component, sampled at uneven time instants $\{t_j\}_{j=1,...,N_{obs}}$. In some applications a training data set of the noise is available. Specifically, let us assume that this training data set $\mathcal{T}_L$ is composed with L time series of the noise $\{X_\ell\}_{\ell=1,...,L}$, sampled at the same time instants $\{t_j\}$. This set can be exploited to improve the control of the FA rate. In this aim, the study [7] considered a standardized periodogram of the form :

$$\widetilde{P}(\nu_k; X_{obs}|S_E, \{X_\ell|S_E\}) := \frac{P(\nu_k; X_{obs}|S)}{\overline{P}_L(\nu_k; \{X_\ell|S_E\})} \quad (2)$$

where

$$\overline{P}_L(\nu_k) := \frac{1}{L}\sum_{\ell=1}^{L}\frac{1}{N}\left|\sum_{j=1}^{N}X_\ell(t_j)e^{-i2\pi\nu_k t_j}\right|^2 \quad (3)$$

is an estimate of the noise PSD. In this setting, [7] shows that $\widetilde{P}$ is independent of the unknown noise PSD and $F(2, 2L)$-distributed. The stochastic estimation noise on the PSD S_E is encapsulated by the parameter L, with of course better detection performances for larger L. Several CFAR detectors can be derived using this standardized periodogram, whose FA rate can be analytically characterized in the case of even time sampling [7]. In the present study, we focus on uneven sampling. We illustrate our study with P as defined by (1) but other periodograms could be used, *e.g.*, [2], [3]. Because of lack of space we consider below only one test, namely the test of the maximum applied to standardized ordinates $[\widetilde{P}_{\nu_1} \ldots \widetilde{P}_{\nu_K}]$.

This test is defined as

$$M(\widetilde{P}) \underset{\mathcal{H}_0}{\overset{\mathcal{H}_1}{\gtrless}} \gamma, \quad \text{with} \quad M(\widetilde{P}) := \max_k \widetilde{P}(\nu_k), \quad (4)$$

and γ is the detection threshold. The associated P_{FA} is defined as :

$$P_{FA}(\gamma; M(\widetilde{P})) := \Pr\left(M(\widetilde{P}) > \gamma | \mathcal{H}_0\right).$$

III. PROPOSED BOOTSTRAP PROCEDURE

Our goal is to obtain a confidence interval for the P_{FA} corresponding to any value of γ. Of course, if we could generate as many realizations as desired of the r.v. $M(\widetilde{P})$ (resulting in, say b, realizations $\{m_i\}_{i=1,...,b}$ of the r.v. M, collected in a vector $\mathbf{m} := [m_1 \ldots m_b]^\top$), we would be able to estimate the empirical distribution of the maximum and thus the P_{FA} by :

$$\widehat{P}_{FA}(\gamma; \mathbf{m}) := 1 - \widehat{\Phi}_M(\gamma; \mathbf{m}), \quad (5)$$

where $\widehat{\Phi}_M$ is the empirical cdf of M, and where the dependency of the estimates on the observed values $\mathbf{m}$ is explicit.

We can not do so however, because the training data set has finite size L. To counteract this fact, we may estimate the parameters of the noise from $\{X_\ell|S_E\}_{\ell=1,...,L}$ under some model, with the aim of generating secondary noise data sets according to this estimated model. We opt for AR models, with PSD :

$$S_{E,AR}(\nu; \boldsymbol{\theta}_{AR}) := \frac{\sigma_o^2}{\left|1+\sum_{j=1}^{o}c_j e^{-2\pi ij\nu}\right|^2}, \quad (6)$$

where $\boldsymbol{\theta}_{AR} := [o\ c_j\ \sigma_o^2]^\top$ is the AR parameter vector (order o, coefficients $\{c_j\}_{j=1,\cdots,o}$ and prediction error variance σ_o^2). Various selection criteria exist to estimate the order (*e.g.*, [14]–[16]). We consider here the Bridge criterion (BC) [16], known to mix the advantages of the Akaike and Bayesian information criteria :

$$\widehat{o} = \arg\min_o BC(o) \quad \text{with} \quad BC(o) := \log\sigma_o^2 + 2\frac{o_M}{N}\sum_{i=1}^{o}\frac{1}{i}, \quad (7)$$

with o_M the largest candidate order and $\widehat{\boldsymbol{\theta}}_{AR} := [\widehat{o}\ \widehat{c}_j\ \widehat{\sigma}_{\widehat{o}}^2]^\top$ the estimated AR parameters, from which a PSD estimate $\widehat{S}_E$ can be obtained as in (6). These parameters also allow to generate $(L+1) \times b$ correlated time series, noted $\{X_\ell|\widehat{S}_E\}$, allowing to generate simulated standardized periodograms $\{\widetilde{P}(\nu_k; X|\widehat{S}_E, \{X_\ell|\widehat{S}_E\})\}$, each requiring 1 time series for numerator (1) and L for denominator (3). The resulting b maxima can be used to estimate the P_{FA} with (5).

However, this estimate is obtained by means of *one* set of AR parameters estimated from $\mathcal{T}_L$. Obviously, we would have obtained a different estimate for a different training set $\mathcal{T}_L$. The question is therefore to know the distribution of this estimate, which we call $\mathcal{D}_{\widehat{P}_{FA}}$ below. The knowledge of this distribution would allow to provide the desired confidence interval. Obtaining $\mathcal{D}_{\widehat{P}_{FA}}$ is not straightforward, however, as only one genuine training set is available. This

is where the bootstrap really comes in : we propose to use the estimated AR coefficients $\{\widehat{c}_j\}$ to generate a number B of fake training data sets, from which we can obtain an estimate of this distribution, $\widehat{\mathcal{D}}_{\widehat{P}_{FA}}$. This leads to the bootstrap procedure, called B_0, described in the Algorithm. It begins by a first AR estimation on $\mathcal{T}_L$ (line 2). Secondary PSD estimates (noted $\widehat{\widehat{S}}_E^{(i)}$, $i = 1, \dots, B$) are generated by reestimating the AR parameters on a i-th fake training data set noted $\{X_\ell|\widehat{S}_E\}$ (for simplicity, we omit the dependence in i in this notation, lines 4-5). These parameters are used to generate b standardized periodograms (line 7-11), the corresponding maxima (line 12) and P_{FA} estimates (line 14). The distribution $\widehat{\mathcal{D}}_{\widehat{P}_{FA}}$ is estimated from the set of B such estimates, $\{\widehat{P}_{FA}^{(i)}\}_{i=1,..,B}$ (line 16). Of course, one advantage of this procedure is that it is independent from the data under test (in contrast to procedures where training data set are not available, and for which the noise statistics must be obtained from the data [17]). An other interesting point is that the marginal distribution of $\widetilde{P}(\nu_k)$ can be estimated for all k, opening the door to tests other than (4) (see [7]). We note, however, that the choice of the parametric model has to be done very cautiously. As in [4], diagnostic plots can be used for model validation.

Algorithm Proposed bootstrap procedure (B_0)

1 **procedure** B_0 ($\mathcal{T}_L$)

2 $\quad \widehat{S}_E(\nu_k; \widehat{\theta}_{AR}(\{X_\ell|S_E\}))$ ▷ 1st PSD estimation (7)

3 $\quad$ **for** $i = 1, \dots, B$ **do**

4 $\quad\quad X_\ell|\widehat{S}_E$ ▷ L time series with PSD $\widehat{S}_E$

5 $\quad\quad \widehat{\widehat{S}}_E^{(i)}(\nu_k; \widehat{\widehat{\theta}}_{AR}(\{X_\ell|\widehat{S}_E\}))$ ▷ 2nd estimation (7)

6 $\quad\quad$ **for** $j = 1, \dots, b$ **do**

7 $\quad\quad\quad X|\widehat{\widehat{S}}_E^{(i)}$ ▷ A time series with PSD $\widehat{\widehat{S}}_E^{(i)}$

8 $\quad\quad\quad P(\nu_k; X|\widehat{\widehat{S}}_E^{(i)})$ ▷ Numerator

9 $\quad\quad\quad X_\ell|\widehat{\widehat{S}}_E^{(i)}$ ▷ L time series with PSD $\widehat{S}_E$

10 $\quad\quad\quad \overline{P}_L(\nu_k; X_\ell|\widehat{\widehat{S}}_E^{(i)})$ ▷ Denominator

11 $\quad\quad\quad \widetilde{P}|\overline{P}_L$ ▷ Standardized periodogram Eq.(2)

12 $\quad\quad\quad m_j^{(i)} = \max_k \widetilde{P}(\nu_k)$ ▷ Max test Eq.(4)

13 $\quad\quad$ **end for**

14 $\quad\quad \widehat{P}_{FA}^{(i)}(\gamma; \mathbf{m}^{(i)})$ ▷ P_{FA} estimate Eq.(5)

15 $\quad$ **end for**

16 $\quad$ **return** $\widehat{\mathcal{D}}_{\widehat{P}_{FA}}(\{\widehat{P}_{FA}^{(i)}\})$ ▷ $\widehat{P}_{FA}$ distribution

17 **end procedure**

IV. USE OF GEV DISTRIBUTIONS

The B_0 procedure above does not rely on any model for the cdf of M, $\widehat{\Phi}_M$, in (5). To be efficient, this estimation requires b to be large, which makes it computationally expensive (see Sec.V-B). However, interesting results from univariate extreme-value theory show that the maximum of a set of identically distributed (dependent or not) r.v. follows a GEV distribution [18]. This suggests that GEV distributions can be used as a model for the cdf of $\max_k \widetilde{P}(\nu_k)$. This method was used in [4] in the case of white noise but we show below that it can also be used in the case of colored noise when a training data set is available, using the considered standardization.

The GEV cdf depends on three parameters, the location $\mu \in \mathbb{R}$, the scale $\sigma \in \mathbb{R}^+$ and the shape $\xi \in \mathbb{R}$:

$$G(m) := \Pr\left(\max_i\{M_i\} \le m\right) = e^{-\left[1+\xi\left(\frac{m-\mu}{\sigma}\right)\right]_+^{-\frac{1}{\xi}}}, \quad (8)$$

with $[x]_+ := \max(0, x)$. In the case $\xi \neq 0$, G is only defined for $m : 1 + \xi\frac{m-\mu}{\sigma} > 0$. In the case $\xi = 0$, G is derived by taking the limit of (8) at 0. In the previous Algorithm, the unknown parameters (ξ, μ, σ) can be estimated using $\mathbf{m}^{(i)}$ (line 12), for instance by maximum likelihood. In this case the maximization can be obtained by an iterative method (see [18]). Denoting by $\widehat{\xi}^{(i)}$, $\widehat{\mu}^{(i)}$, and $\widehat{\sigma}^{(i)}$ the estimated GEV parameters, $\widehat{P}_{FA}^{(i)}$ can be estimated as in (5). The estimated threshold associated to a target P_{FA} can be computed from (5) and (8) as :

$$\widehat{\gamma}^{(i)}(P_{FA}) = \widehat{\mu}^{(i)} - \frac{\widehat{\sigma}^{(i)}}{\widehat{\xi}^{(i)}}\left(1 - \{-\log(1 - P_{FA})\}^{-\widehat{\xi}^{(i)}}\right)$$

for $\xi \neq 0$. In the following, we will note by $\mathsf{B}^\star$ the B_0 procedure using the GEV model.

V. NUMERICAL RESULTS

The first results are obtained using a synthetic colored noise in order to analyze and validate the B_0 procedure (Sec. V-A) and its "GEV-based" form (Sec. V-B). Sec. V-C presents an application involving real solar data standardized by hydrodynamic simulations (HDS) of the Sun.

V-A. Proposed bootstrap method B_0

We first consider a synthetic colored noise, E, as an AR(6) process with coefficients $c = \{0.7, 0.05, 0, 0.3, 0, -0.3\}$. The theoretical PSD S_E is given by (6). It is represented by the green curve in the panels a) and b) of Fig.1. For the uneven sampling, we consider a regular grid $\{t_k := k\Delta t\}_{k=1,..,N}$ with $N = 1024$ and $\Delta t = 1$, from which we randomly select $N = 103$ data points. The first row of Fig.1 illustrates a snapshot of B_0 (see Algorithm). We generate $L = 20$ synthetic time series following the true PSD S_E, noted $\{X_\ell|S_E\}$, from which we can compute an averaged periodogram $\overline{P}_L|S_E$ (panel a), black solid line). The dashed red curve in panel a) illustrates the primary parametric PSD estimate $\widehat{S}_E$ obtained from $\{X_\ell|S_E\}$ using the BC criterion given in (7). In panel b), the blue dashed line illustrates one

secondary PSD estimate $\widehat{\widehat{S}}_E^{(i)}$ obtained from a 'fake training data set' $\{X_\ell | \widehat{S}_E\}$ of L simulated time series. This panel also shows for comparison with a) the averaged periodogram $\overline{P}_L | \widehat{S}_E$ (red solid line). Panel c) displays one standardized periodogram obtained from $L + 1$ series $\{X_\ell \widehat{\widehat{S}}_E^{(i)}\}$, with the maximum value $m_j^{(i)}$ indicated by the red circle. In this simulation, we obtain $B = 5200$ estimates $\widehat{P}_{FA}^{(i)}(\gamma)$ as in (5) (grey curves in d). The true P_{FA} (more precisely an accurate estimation obtained through 10^5 MC simulations of the true AR process) is shown in green. We see that the estimates bound the true P_{FA} over the whole γ range.

In the inset panel e), we compare with a classical P_{FA} bootstrap estimation procedure that would ignore noise correlations and use the Generalized Lomb Scargle periodogram (P_{GLS}) [3], a periodogram frequently used in Astronomy. In this procedure, we generate unevenly sampled light curves by resampling the data (through random permutations), evaluate the P_{GLS}, compute the maximum and perform test (4) with $\widetilde{P} | \overline{P}_L$ replaced by $\widetilde{P}_{GLS} | \widehat{\sigma}_W^2 := P_{GLS} / \widehat{\sigma}_W^2$ with $\widehat{\sigma}_W^2$ the variance estimated from the data. This provides one estimate $\widehat{P}_{FA}(\gamma)$ and we repeat this experiment 10^3 times. The resulting curves $\widehat{P}_{FA}(\gamma)$ are plotted in black. The true P_{FA} of this procedure (in red) has been generated with 10^5 MC simulations. The method fails to estimate accurately the FA rate, because this simple resampling by permutation breaks the data correlation. This is in clear contrast with the procedure shown in d), which takes benefit from the training data set.

Panel f) shows, in grey, the distribution $\widehat{\mathcal{D}}_{\widehat{P}_{FA}}(\mathsf{B}_0)$ for a threshold fixed at $\gamma_F = 10.6$ corresponding to a true P_{FA} of 0.1 (green). We see that the estimates bound the true value with a relatively small dispersion. The 95% confidence interval, obtained from the Gaussian approximation (red), is indicated in blue and indeed contains the true P_{FA}.

V-B. Use of the GEV distribution

In practice, one limitation of the B_0 procedure is its computation time, related in particular to the large number (b) of periodogram maxima required for the estimation to be accurate. To reduce b while keeping a tight confidence interval for the P_{FA}, we consider applying the version of the bootstrap procedure using the GEV approximation ($\mathsf{B}^\star$). The left panel of Fig.2 compares, as a function of b, the empirical means (solid lines, right ordinate axis) and dispersions (dashed lines, left ordinate axis) for the distributions of the FA estimates by three methods (see legend) when the test is ran at a true P_{FA} of 0.1. All procedures lead to a decreasing dispersion and bias in the mean as b increases, with similar estimation performances for $\mathcal{D}_{\widehat{P}_{FA}}$ and $\widehat{\mathcal{D}}_{\widehat{P}_{FA}}$ (respectively in black and green), although for the latter only one genuine set $\mathcal{T}_L$ is available. Even more interestingly, these results show that the lowest dispersion and bias for the mean $P_{FA} = 0.1$ is obtained by the third method ($\mathsf{B}^\star$), because the GEV model is indeed appropriate and has far
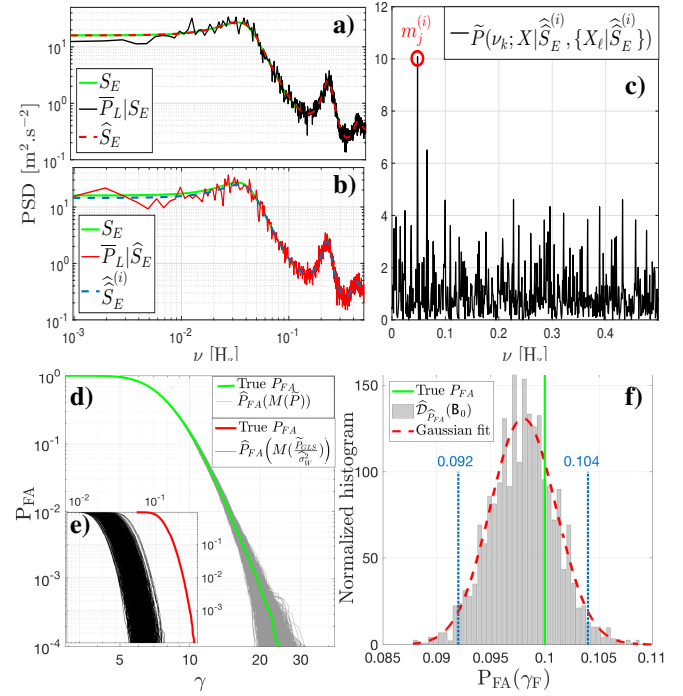

Fig. 1. Top : Snapshots of the B_0 procedure for an AR(6). Bottom : $\widehat{P}_{FA}$ vs P_{FA} for several bootstrap methods.

less degrees of freedom than the non parametric estimate $\widehat{\Phi}_M$ used in the two other bootstraps. The right panel compares the possible compromises dispersion *vs* computation time for B_0 and $\mathsf{B}^\star$. We see that $\mathsf{B}^\star$ allows for better compromises, with a $\approx 20 - 40\%$ lower dispersion than B_0 at the same computational cost.

V-C. Application to exoplanet detection

As in [7], an application of this work is the detection of exoplanetary signatures in the noise of RV data. In short, orbiting planets create, through the gravitational force, a quasi-periodic Doppler shift in the stellar light, leading to so-called RV time series. The stellar surface of solar-like stars are convectively unstable. Convection is a stationary stochastic process which generates (large) fluctuations around the hydrostatic equilibrium of the star. HDS of the inhomogeneous pattern (called granulation) have been substantially improved in the last decade [19] offering the opportunity to generate simulated time series (yet few, owing to the computational cost of the HDS), that can be used as a training data set $\mathcal{T}_L$.

We consider here solar RV data acquired by the GOLF spectrophotometer on board SoHo satellite [20]. The periodogram of 30h observations is shown in the inset panel of Fig.3 (top, black). Different phenomena occur depending on the considered frequency. Here, we focus only on the granulation noise, which is active over minutes to days (grey shaded region) corresponding to the temporal scale of close-in planets. As an illustration of HDS, we show an averaged periodogram $\overline{\mathbf{P}}_L$ obtained through $L = 6$ independent HDS of the granulation solar noise [21], covering the frequency range associated to periods of 10 min to 1 day (red).

For our experiment, we introduce in the data a fake periodic signal : $s(t) = A \sin(2\pi t \nu_s)$, with $A = 0.28$ m.s^{-1}, $\nu_s = 0.046$
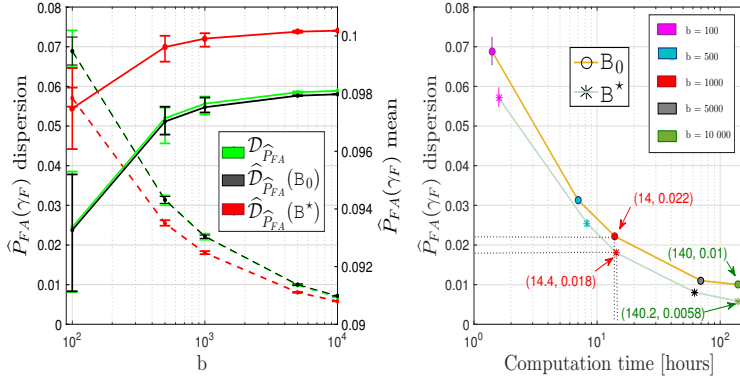
Fig. 2. Comparison between the B_0 and $B^\star$ procedures.

Fig. 3. Illustration of the B_0 procedure on real solar data.

mHz (for these data, $\frac{A}{\sigma_{X_{obs}}} \approx 0.22$). This situation corresponds to a Keplerian signature of a 0.27 Earth-mass planet, orbiting a Sun-like star with circular orbit and period of 6h. The left panel of Fig.3 displays $\widetilde{P}$ obtained from evenly sampled data (see title). In this case the P_{FA} of test (4) is given Eq.(18) of [7]. The theoretical (asymptotically exact) thresholds corresponding to three target P_{FA} (respectively, 0.1, 0.5 and 0.9) are indicated by the black horizontal (respectively dotted, dash-dotted and dashed) lines. The color dashed lines indicate the $\approx 95\%$ confidence intervals obtained by B_0 for the three thresholds. Comparing with the black lines shows that the bootstrap method works well. Similar results are obtained in the case of uneven sampling (right panel), where the data is obtained by randomly selecting $N = 30$ samples of the evenly sampled time series. The corresponding spectral window (modulus of the Fourier Transform of the observation window) is plotted in grey in the inset panel.

VI. CONCLUSIONS

This paper has investigated the possibility of using noise training data sets to improve the control of the false alarm rate associated to detection tests. This method is based on standardized periodograms, which have been considered in a previous study [7] but in the case of regularly sampled observations. By developing an adapted bootstrap procedure in the Fourier domain, it appears that one can reliably bound the false alarm probability in the general case of irregularly sampled observations. However, as this procedure is based on MC simulations, it is computationally heavy. Exploiting a GEV distribution allows to save time while keeping the same behavior for the resulting FA estimates. This procedure can be useful for the detection of extrasolar planets in RV data. In this case, the time sampling is often uneven, the exoplanetary signatures hidden in the colored noise coming for the stellar surface convection and this noise can be simulated using astrophysical codes.
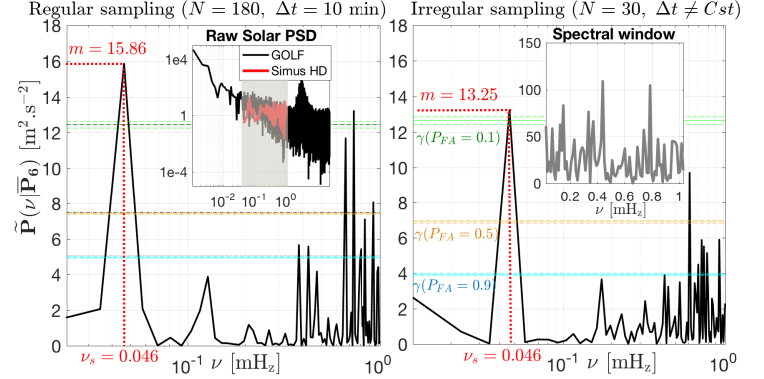
REFERENCES

[1] A. Schuster, "On the investigation of hidden periodicities," *J. Geophys. Res.*, vol. 3, pp. 13, 1898.

[2] J.D. Scargle, "Studies in astronomical time series analysis. II - Statistical aspects of spectral analysis of unevenly spaced data," *ApJ*, vol. 263, pp. 835–853, 1982.

[3] M. Zechmeister and M. Kürster, "The generalised Lomb-Scargle periodogram. A new formalism for the floating-mean and Keplerian periodograms," *A&A*, vol. 496, pp. 577–584, 2009.

[4] M. Süveges, "Extreme-value modelling for the significance assessment of periodogram peaks," *MNRAS*, vol. 440, pp. 2099–2114, 2014.

[5] J.H. Horne and S.L. Baliunas, "A prescription for period analysis of unevenly sampled time series," *ApJ*, vol. 302, pp. 757–763, 1986.

[6] F.A.M. Frescura et al., "Significance of periodogram peaks and a pulsation mode analysis of the beta cephei star v403 car," *MNRAS*, vol. 388, no. 4, pp. 1693, 2008.

[7] S. Sulis, D. Mary, and L. Bigot, "A study of periodograms standardized using training data sets and application to exoplanet detection," *IEEE Trans. SP.*, vol. 65, pp. 2136–2150, 2017.

[8] A.M. Zoubir and R.D. Iskander, *Bootstrap Techniques for Signal Processing*, Cambridge Univ. Press, 2004.

[9] E. Paparoditis and D. Politis, "The local bootstrap for periodogram statistics," *J. Time Series Analysis*, vol. 20, no. 2, pp. 193–222, 1999.

[10] D. Politis and J. Romano, "The stationary bootstrap," *JASA*, vol. 89, pp. 1303–1313, 1994.

[11] J.P. Kreiss and E. Paparoditis, "Autoregressive-aided periodogram bootstrap for time series," *Ann. Statist.*, vol. 31, pp. 1923–55, 2003.

[12] X. Shao, "The dependent wild bootstrap," *JASA*, vol. 105, pp. 218–235, 2010.

[13] G. Young, "Bootstrap : More than a stab in the dark ?," *Statist. Sci.*, vol. 9, pp. 382–395, 1994.

[14] H. Akaike, "Fitting autoregressive models for prediction," *Ann. Math. Statist.*, vol. 21, pp. 243–247, 1969.

[15] J. Rissanen, "Universal coding, information prediction and estimation," *Trans. Inf. Theory*, pp. 629–636, 1984.

[16] J. Ding et al., "Bridging AIC and BIC : a new criterion for autoregression," *ArXiv e-prints*, 2015.

[17] M.B. Priestley, *Spectral Analysis and Time Series*, Acad. Press, 1981.

[18] S. G. Coles, *An Introduction to Statistical Modelling of Extreme Values*, Springer-Verlag, London, 2001.

[19] Å. Nordlund et al., "Solar Surface Convection," *Living Reviews in Solar Physics*, vol. 6, pp. 2, 2009.

[20] R.A. Garcia et al., "Global solar Doppler velocity determination with the GOLF/SoHO instrument," *A&A*, vol. 442, pp. 385–395, 2005.

[21] L. Bigot and F. Thévenin, "3d hydrodynamical simulations of stellar surfaces : Applications to gaia," in *SF2A*, 2008, p. 3.